



Performance Evaluation of Successive Interference Cancellation on Gain Ratio Power Allocation using Underwater Visible Light Communication Channel

Luthfi Nur'Adli^{a,*}, Arfianto Fahmi^a, Brian Pamukti^a

^a School of Electrical Engineering, Telkom University, Telekomunikasi No.1, Bandung, 40257, Indonesia

Corresponding author: *luthfinuradli@student.telkomuniversity.ac.id

Abstract— Underwater Visible light communication (UVLC) is a network communication wirelessly where information is transmitted employing light through visible waves; in this case, the light source comes from a light-emitting diode (LED) as a transmitter underwater. VLC has several advantages over radio frequency technology, such as safer communication because light propagation cannot penetrate the wall, so it is difficult to do hacking, easy to get a license, relatively build cheap cost, and has no side effects on health. However, VLC has several limitations, one of which is the narrow bandwidth modulation. VLC undergoes a distribution of modulated bandwidth to allocate against each user. This bandwidth sharing has an impact on reduced system capacity. This study applied non-orthogonal multiple access (NOMA) to increase system capacity. This research analyzes the performance of the two best power allocation methods in a water medium, including gain ratio power allocation (GRPA) and static power allocation (SPA). In the results obtained in the NOMA-UVLC power allocation value, GRPA is more stable than SPA power allocation. Then applying residue in the successive interference cancellation (SIC) process will result in a decrease in system capacity compared to no residue in the SIC process. This study found that the GRPA power allocation is more stable in capacity performance compared to the application of SPA power allocation. Average capacity increase of 48.5% in GRPA power allocation.

Keywords— Underwater visible light communication; NOMA; GRPA; SPA; successive interference cancellation.

Manuscript received 12 Jan. 2022; revised 5 Mar. 2022; accepted 22 Apr. 2022. Date of publication 30 Jun. 2022.
International Journal on Informatics Visualization is licensed under a Creative Commons Attribution-Share Alike 4.0 International License.



I. INTRODUCTION

The development of the times is increasing in direct proportion to the development of technology. Currently, one of the technologies being developed is the communication between systems and networks without using cables, commonly referred to as wireless networks. This network can connect multiple devices such as smartphones, laptops, computers, and other electronic devices. This wireless network is usually used for transmission media such as microwaves, radio waves, and light waves [1]. Currently, the demand for the use of wireless network services, especially in medium water, continues to increase. For this reason, light wave-based wireless network technology is one solution to overcome this [2].

Visible Light Communication (VLC) or known as visible light communication, is a wireless network communication where information is transmitted by light media via visible waves, in this case the light source comes from a Light

Emitting Diode (LED) [3]. This VLC technology uses visible light which has a wavelength of 375-780 nm and a frequency of 400-800 THz [4]. VLC has better speed and capacity than Radio Frequency (RF). In addition, VLC has several advantages over RF technology such as safer communication because light cannot penetrate walls making it difficult to hack, easy to get a license, relatively cheap manufacturing costs and no side effects on health. But VLC has a drawback, namely the narrow modulation bandwidth so that it lacks system capacity [5].

Pamukti et al [6] have examined NOMA with the proposed Water-Filling Random Resource Allocation (WFRR) which combines power and code domains. Simulations have been conducted with a user count of up to 40 to get the ideal conditions. Some of the test parameters that have been done are Fairness Index, Probability user, Average Datarate and Energy Savings. By prioritizing energy issues, the results of the study showed that energy saving could increase by 46% compared to without WFRR. In addition, the power

allocation is done not using SPA or GRPA but using the Water Filling (WF) approach.

To overcome the limited bandwidth modulation on performance in the VLC system, non-orthogonal multiple access (NOMA) is applied to the downlink of the VLC network to increase the total data performance effectively. Based on the previous NOMA-VLC research [3], the study was conducted by analyzing the performance of power allocation gain ratio power allocation (GRPA) in open spaces. The results show that GRPA significantly increases performance in terms of sum-rate and user justice compared to static power allocation (SPA) in open spaces [7].

VLC technology is currently being developed for its application in the medium of water or in open spaces [8]. Underwater visible light communication (UVLC) is a development of VLC, which is a communication system technology that can convey data by regulating visible light in the water as a whole [9]. This UVLC working model communicates submerged data signals by considering wave height, absorption, and wind speed, each of which has an alternative coefficient [10]. The effect of water type in UVLC communication is separated into four types of water, namely seaside water, estuary waters, clear sea water, and pure seawater [4].

This research analyses the performance of the two best power allocation methods in the water medium, including gain ratio power allocation (GRPA) and static power allocation (SPA). In the results obtained in the NOMA-UVLC power allocation value, GRPA is more stable than SPA power allocation. Then applying residue in the successive interference cancellation (SIC) process will result in a decrease in system capacity compared to no residue in the SIC process. This study found that the GRPA power allocation is more stable in capacity performance compared to the application of SPA power allocation. Average capacity increase of 48.5% in GRPA power allocation.

This research consists of five chapters. Chapter II describes research related to the methods used in the simulation process and describes the system model. Chapter III calculates the parameters in the form of distance to the receiver position, system capacity, and signal to interference plus noise ratio (SINR) values using computer simulations for each scenario. Chapter IV describes the analysis of the results of the calculations that have been carried out. Chapter V explains the conclusions from the simulation results.

II. MATERIALS AND METHOD

A. Research Flowchart

Figure 1 shows the stream graph of the NOMA-UVLC system did in the simulation. In this simulation, the LED discharges light and communicates an electrical signal. This modeling process is the stage when simulating by building a system model on NOMA-UVLC with component parameters to be determined. After that, calculate the Signal to Interference Plus Noise Ratio (SINR) and Capacity. This modeling process is the stage when simulating by building a model system on NOMA-UVLC with component parameters to be determined. In the process of designing a system model, it is to create a system model according to a predetermined block diagram. In the process of determining this parameter is

an input diagram for determining the parameters that have been calculated, namely the distance. In this process, diagram is the calculation of SINR and Capacity manually without using the help of software that has become the reference for the next step.

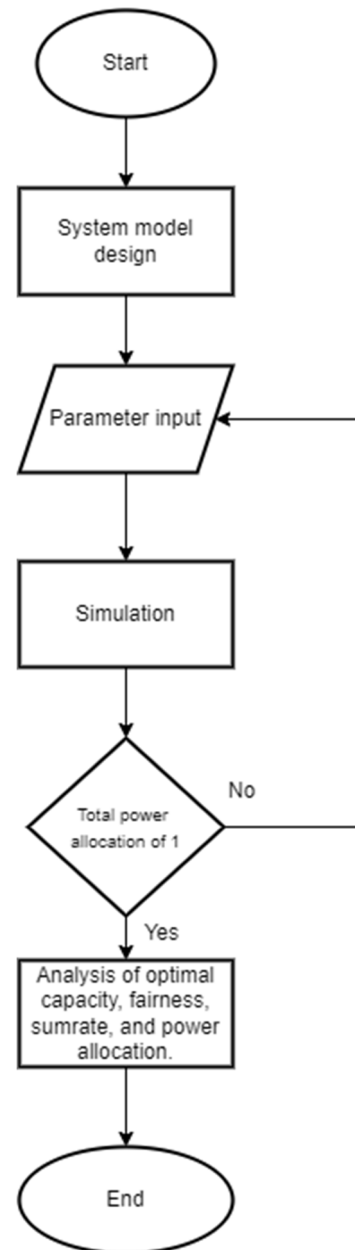


Fig. 1 Simulation Flowchart for Research.

In this simulation process, two scenarios are performed by testing the performance of power allocation on the NOMA-UVLC system. Where the first scenario compares the optimal allocation between the SPA allocation and the GRPA allocation. Then the second scenario tests the fairness of each user to the sumrate on the NOMA-UVLC system. After that, a comparison graph is made between the two different power allocations so that the differences in the values of the other parameters can be seen. In designing the NOMA-UVLC System in this research, several input parameters are given to the system, which will affect the simulation results. The input parameters used in this simulation are listed in Table I.

TABLE I
WATER TYPE

Water Type	$a(m^{-1})$	$b(m^{-1})$	$c(m^{-1})$	Operating Wavelength
Pure Water	0.114	0.037	0.151	450 – 570 mm
Coastal Ocean	0.179	0.220	0.339	520 – 570 mm
Turbid Harbor	0.366	1.829	2.195	520 – 570 mm

B. Data Collection Method

In the research simulation on NOMA-UVLC as shown in Figure 2, wherein the image, there is one LED as a transmitter and also as a light source. On the receiving side, four photodetectors are used in each scenario. In determining the position of the required distance information between the transmitter and receiver. The LED is protected by a glass tube covered with a rope in seawater from a ship [26]. The scenario uses a channel in the form of a LOS channel so that no obstacle angle affects the process of sending information.

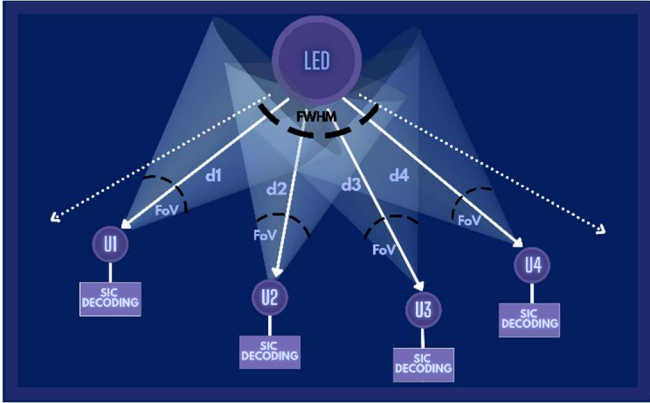


Fig. 2 NOMA-UVLC System Design with 4 Users on LOS Channel Model.

C. Channel Model

VLC technology is currently being developed for its application in the medium of water or in open spaces. Underwater visible light communication (UVLC) is a development of VLC, a communication system technology that can convey data by regulating visible light in the water as a whole [11]. This UVLC working model communicates a submerged data signal by considering wave height, absorption, and wind speed, each of which has an alternative coefficient. The effect of water type in UVLC communication is separated into four types of water, namely seaside water, estuarine waters, clear sea water, and pure seawater [12].

The types of water that have been mentioned have different scatterings, such as pure sea water having Rayleigh scattering. Because the frequency in pure seawater is more limited because it contains salt and particles in it. In UVLC system has a propagation loss factor [6]. This propagation loss factor is caused by the beam extinction coefficient, which has the following equation [12].

$$c(\lambda) = a(\lambda) + b(\lambda), \quad (1)$$

from equation 1, we get $a(\lambda)$ is the absorption coefficient in seawater and $b(\lambda)$ is the rayleigh scattering coefficient for clear seawater. To get the propagation loss factor value with the following formula [13],

$$Lp = \exp^{-c(\lambda).d}, \quad (2)$$

where respect to the data from the propagation loss equation, for $c(\lambda)$ the beam extinction coefficient is the visible light frequency, and d is the distance.

The line of sight (LOS) propagation channel model is used in this simulation. The LOS propagation channel model allows the transmission of information without any barriers or obstructions. This propagation channel model is very good to be used for research on VLC technology because there are no barriers [14]. It takes less energy diffuse, and the percentage of system reliability is guaranteed compared to non-line of sight (NLOS) propagation channels [15]. However, it is rare to find a propagation channel like this at the implementation stage in the real world. The formula for calculating channel gain in this LOS propagation channel model can generally be seen in the following formula [16]:

$$h_{los} = \frac{A_r(m+1)}{2\pi d^2} \cos^m(\phi) T_s(\psi) g(\psi) \cos(\psi), \quad (3)$$

when the information that $A_r, d, \phi,$ and ψ are the photodetector area, the distance between the LED and the receiver, the irradiation angle at the transmitter, and the receiver angle at the receiver, while $g(\psi)$ is the optical concentrator, $T_s(\psi)$ is the gain on the optical filter, and m is the angular distribution of the radiation intensity pattern modeled using the Lambertian emission intensity, in general it can be expressed in the following formula [13]:

$$m = \frac{-\log_{10} 2}{\log_{10} \cos \phi_{1/2}}, \quad (4)$$

where m is the Lambertian equation and $\phi_{1/2}$ is the semi-angle or full width at half maximum (FWHM) value on the LED.

D. Power Allocation

In the application of the NOMA-UVLC system on the sending side, superposition coding is applied which has a function for power allocation and signal merging modeling based on channel gain for each user [17]. In the NOMA downlink power allocation has a symbol with α [18]. On the principle of the NOMA-UVLC system in regulating the allocation of power sent by the LED, it is adjusted according to the channel gain conditions of each user [19]. In this simulation, 2 types of power allocation are used, including gain ratio power allocation (GRPA) and static power allocation (SPA) [20].

In GRPA power allocation, it is a power allocation technique involving the channel gain value from other users to the user- n [21]. In this simulation using 4 users. Mathematically the calculation of finding the GRPA value can be expressed in the following equation [22]:

$$\alpha_k = \frac{\frac{h_1}{h_k}}{1 + \frac{h_1}{h_2} + \dots + \frac{h_1}{h_k}}, \quad 2 \leq k \leq K. \quad (5)$$

In power allocation, SPA is a power allocation technique by randomly assigning α value with power allocation to the user manually according to the user's channel conditions.

E. Signal to Interference Plus Noise Ratio (SINR)

Figures Signal to interference plus noise ratio (SINR) is a value that compares the value of the noise that occurs in the system and the transmitted signal against interference [23]. Signal processing will be very disturbed when sending information when there is interference and noise [11]. When the interference value is received (I_p), and the noise (N_p) is received at the receiver side, the larger it will affect the information signal that has been received, the smaller it will be [24]. Mathematically, SINR can be expressed in the following equation [24]:

$$SINR = \frac{S_P}{I_p + N_P}. \quad (6)$$

In the VLC-NOMA system with a downlink scheme, when the SIC is operating and does not experience residue or so-called perfect SIC. It can be interpreted that all power allocations that are not calculated for the user- n have been successfully canceled. Mathematically, the SINR that does not experience residue can be obtained from the following equation [24]:

$$SINR_n = \frac{h_n^2 \cdot P_n}{h_n^2 \cdot \sum_{k=n}^N P_k + \sigma^2}, \quad (7)$$

where P_n is the n th user power allocation, and σ^2 is the total thermal noise and shot noise.

Whereas in the NOMA-UVLC system with a downlink scheme, when the SIC is operating and experiencing residues or commonly called imperfect SIC, it can be interpreted that power allocation that is not calculated to the user- n is not completely canceled and is considered as interference. Mathematically, the SINR with residue can be obtained from the equation as follows [24]:

$$SINR_n = \frac{h_n^2 \cdot P_n}{h_n^2 \cdot \sum_{k=n}^N P_k + \varepsilon \cdot h_n^2 \cdot \sum_{k=n-1}^{n-1} P_k + \sigma^2}, \quad (8)$$

where ε is the percentage of residue that occurs in the SIC process or commonly called the interference cancellation factor.

F. Capacity

Capacity is a parameter that states the maximum bit rate per second sent from the transmitter to each receiver in the data transmission process. Capacity can be obtained from calculations using the Shannon capacity theorem, which can be written with the following equation [25]:

$$r_n = B \cdot \log(1 + SINR_n), \quad (9)$$

where B is the bandwidth value and $SINR$ is the SINR parameter value for each user.

III. RESULTS AND DISCUSSION

This part shows the experimental outcomes in view of predefined parameter:

TABLE II
SIMULATION INPUT PARAMETERS.

Parameter	Value
Transmitter Type	LED
Amount	1 Piece
Power	5 Watt
Bandwith	10 Mhz

Receiver	Photodiode Type	PIN
	Detector Area Photodiode	100 mm^2
	Field of View (FoV)	77°
	Responsivitas (A/W)	0.6
	Depth	10 m
	Optical Concentrator's Refractive Index	1.5
Others	Rayleigh Scattering Value (Pure Water)	0.0022 m^{-1}
	Seawater Absorption Value (Pure Water)	0.114 m^{-1}

A. Research Scenario

The first scenario is a network quality simulation by comparing the best power allocation performance quality between GRPA and SPA power allocations on the successive interference cancellation (SIC) side without getting a residue. It is assumed that another lightless propagation is sent from the LED to the photodetector at the receiving end. Then using pure seawater, an optical concentrator, and a scenario of 4 users with the distance of each user from the LED lights as shown in Table III.

TABLE III
SCENARIO 4 USER POSITION

User	Distance (m)	Power Allocation SPA	Power Allocation GRPA
1	3.0	$\alpha_1 = 2.050 \cdot 10^{-1}$	By channel value
2	2.9	$\alpha_2 = 2.425 \cdot 10^{-1}$	
3	2.8	$\alpha_3 = 2.675 \cdot 10^{-1}$	
4	2.7	$\alpha_4 = 2.850 \cdot 10^{-1}$	

This simulation uses the NOMA system with the sending side applied superposition coding that contains the power allocation for each user. This scenario compares power allocation methods, including gain ratio power allocation (GRPA) with static power allocation (SPA). The discovery and real values are displayed in Table IV.

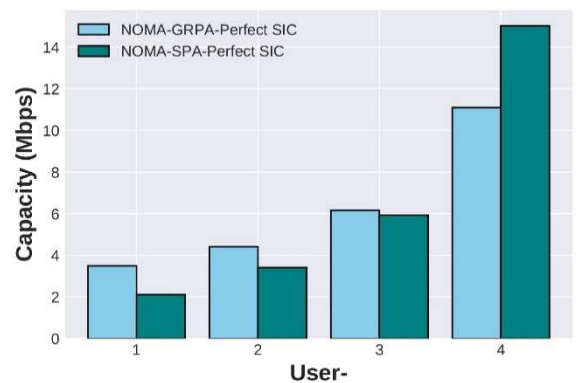


Fig. 3 Power Allocation Performance in Perfect SIC Conditions.

TABLE IV
CAPACITY VALUE IN THE FIRST SCENARIO

User	Distance (m)	Capacity (Mbps)	
		GRPA	SPA
1	3.0	3.51	2.11
2	2.9	4.41	3.41
3	2.8	6.15	5.93
4	2.7	11.09	15.02

We considered changing the residue obtained at the receiving end of the SIC. In the second scenario, we simulate the network quality by comparing the best power allocation performance quality between GRPA and SPA on successive interference cancellations (SIC) by obtaining residuals. It can also be called imperfect SIC. The discovery and real values are displayed in Table V.

TABLE V
CAPACITY VALUE IN THE SECOND SCENARIO

User	Distance (m)	GRPA		SPA	
		Power Allocation	Capacity (Mbps)	Power Allocation	Capacity (Mbps)
1	3.0	0.324	3.51	0.285	2.11
2	2.9	0.271	4.41	0.267	3.41
3	2.8	0.223	6.15	0.242	5.93
4	2.7	0.180	11.0	0.205	15.0

After doing the second scenario, we get the output that when the first scenario using perfect sic produces a higher NOMA-UVLC system capacity value than in the second scenario using imperfect sic. This is because in imperfect sic there is a residue with a residual value of 0.1 while in perfect sic there is no residue in the system [2]. The results of the comparison of the two scenarios can be seen in Table VI.

TABLE VI
CAPACITY VALUE WITH SIC EFFECT

User	Distance (m)	Perfect SIC		Imperfect SIC	
		GRPA	SPA	GRPA	SPA
1	3.0	3.51	2.11	3.51	2.11
2	2.9	4.41	3.41	4.26	3.35
3	2.8	6.15	5.93	5.71	5.56
4	2.7	11.09	15.02	9.56	13.36

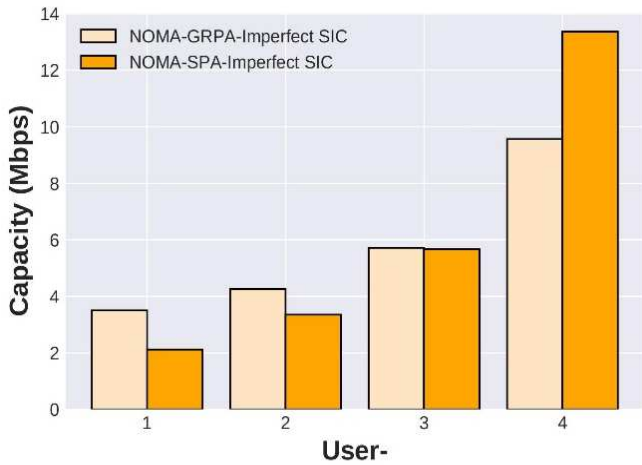


Fig. 4 Power Allocation Performance in Imperfect SIC Conditions.

B. Power Allocation

This analysis aims to compare the power allocation results from the two scenarios that have been carried out. This simulation is used on the receiving side by implementing SIC for the NOMA-UVLC system with the application of GRPA and SPA power allocation methods. Then it is assumed that the SIC does not experience residue with the design specifications of the user's position having different distances from each LED which can be seen in Table II. Based on the simulation results in Figure 3, there is an increase in system

capacity performance as the user's distance increases to the coverage of one LED.

In the first scenario with the application of GRPA power allocation, the 1st user gets a capacity value of 3.5 Mbps, while for the SPA power allocation, it gets 2.1 Mbps. There is a difference in the capacity value of 1.4 Mbps. In the 2nd user the capacity value obtained is higher than the 1st user with a value of 4.4 Mbps for GRPA power allocation and 3.4 Mbps for SPA power allocation. The 3rd user gets a capacity value of 6.1 Mbps for GRPA power allocation, while for SPA power allocation it is 5.9 Mbps. On the 4th user, the SPA power allocation resulted in a higher capacity value than the GRPA power allocation with a difference of 4 Mbps. The capacity value has increased as can be seen in Figure 3 showing that the closer the user is to the coverage of one LED, the system capacity will increase. The results obtained that the capacity of the 1st, 2nd, and 3rd users of the GRPA power allocation has a higher value than the SPA power allocation. Meanwhile, on the 4th user, the SPA power allocation has a higher value than the GRPA power allocation.

In this second scenario, the NOMA-UVLC system when in the process of canceling the signal at the receiver side there is a residue, then the cancellation process can be interpreted as an imperfect SIC. In this simulation, it is assumed that the residual value is 0.1 in the system. Based on the simulation results in Figure 4, there is an increase in system capacity performance in the imperfect SIC along with the increase in user distance to the coverage of one LED. The results obtained that the capacity of the 1st, 2nd, and 3rd users of the GRPA power allocation has a higher value than the SPA power allocation. Meanwhile, on the 4th user, the SPA power allocation has a higher value than the GRPA power allocation. The capacity value has increased as can be seen in Figure 3 showing that the closer the user is to the coverage of one LED, the system capacity will increase.

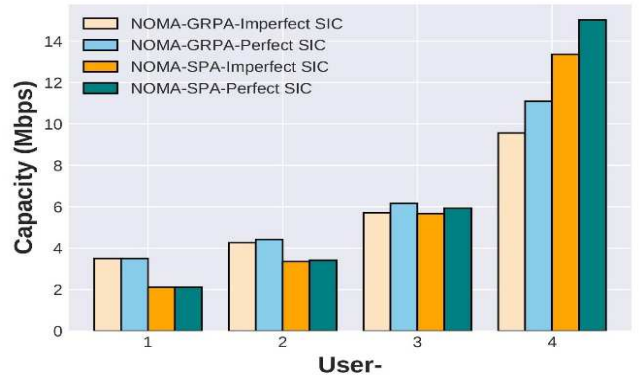


Fig. 5 Effect of Residual Increase.

C. Analysis of the Effect of Imperfect SIC on the Capacity of the NOMA-UVLC System

This simulation analyzes the effect of residual (ϵ) generated by the signal cancellation process on the receiving side as shown in Figure 5. With the application of perfect SIC in GRPA power allocation, the 4th user gets a capacity value of 11.09 Mbps, while for perfect SIC in GRPA power allocation, it gets 9.5 Mbps. From these results, it can be seen that when the imperfect SIC condition ($\epsilon = 0.1$) occurs, there is a decrease in capacity performance of 4.7% from the perfect SIC condition ($\epsilon = 0$) at the 4th user position. The residual

increase from 0 to 0.1 in the NOMA-UVLC can affect the decrease in capacity values. This is because when the signal cancellation process on the receiving side produces residues considered as interference, it impacts SINR performance and capacity for each user in the NOMA-UVLC system model.

IV. CONCLUSION

Based on the simulation results and research analysis regarding the comparison of the performance of power allocation gain ratio power allocation (GRPA) with static power allocation (SPA) in the NOMA-UVLC system with LOS channels carried out in this simulation, several conclusions can be drawn. Based on the NOMA-UVLC system model's performance, power allocation changes can affect system capacity performance. This study found that the GRPA power allocation is more stable in capacity performance compared to the application of SPA power allocation. The average capacity increase is 48.5% in the GRPA power allocation. This is influenced by the fact that the GRPA power allocation is obtained by first calculating using a comparison ratio by considering the gain channel for each user. In comparison, the SPA power allocation is obtained by manually determining which takes into account the channel conditions for each user. So that the GRPA power allocation is more suitable to be applied in dynamic users, while the SPA power allocation is more suitable to be applied in static users.

When the NOMA-UVLC system model is applied to imperfect SIC conditions, the average capacity performance decreases by 6.8% from perfect SIC conditions with GRPA power allocation. This is due to the residue contained in the imperfect SIC condition of 0.1. The NOMA-UVLC system model residue is considered interference in the signal cancellation process at the receiver side.

Based on the conclusions in this research, several things allow it to be developed in further research. The suggestions that can be developed are as follows, perform simulations and analyzes on various types of optimal modulation in the NOMA-UVLC system model, making prototypes for the NOMA-UVLC system model so that it can be applied in life, and conduct research on the relationship between optical concentrator and its effect on NOMA-UVLC performance.

ACKNOWLEDGMENT

We thank the Optical Communication Laboratory and Telkom University for helping with this research.

REFERENCES

- [1] M. Farhan, D. Darlis, and A. Ramdhan, "Perancangan Dan Implementasi Komunikasi Suara Pada Sistem Bi-directional Underwater Visible Light Communication Menggunakan Led Biru | Farhan | eProceedings of Applied Science." <https://openlibrarypublications.telkomuniversity.ac.id/index.php/appliedscience/article/view/7450> (accessed Jun. 07, 2022).
- [2] L. E. M. Matheus, A. B. Vieira, L. F. M. Vieira, M. A. M. Vieira, and O. Gnawali, "Visible Light Communication: Concepts, Applications and Challenges," *IEEE Communications Surveys and Tutorials*, vol. 21, no. 4, pp. 3204–3237, Oct. 2019, doi: 10.1109/COMST.2019.2913348.
- [3] M. Figueiredo, L. N. Alves, and C. Ribeiro, "Lighting the Wireless World: The Promise and Challenges of Visible Light Communication," *IEEE Consumer Electronics Magazine*, vol. 6, no. 4, pp. 28–37, Oct. 2017, doi: 10.1109/MCE.2017.2714721.
- [4] R. Mulyawan et al., "A comparative study of optical concentrators for visible light communications," <https://doi.org/10.1117/12.2252355>, vol. 10128, pp. 142–147, Jan. 2017, doi: 10.1117/12.2252355.
- [5] H. Marshoud, V. M. Kapinas, G. K. Karagiannidis, and S. Muhaidat, "Non-orthogonal multiple access for visible light communications," *IEEE Photonics Technology Letters*, vol. 28, no. 1, pp. 51–54, Sep. 2015, doi: 10.1109/LPT.2015.2479600.
- [6] B. Pamukti, V. S. WP, A. Fahmi, N. M. Ardiansyah, and N. Andini, "Analysis of water-filling random resource allocation (w-frra) for energi saving in light fidelity (lifi)." *Engineering Letters*, vol. 28, No. 4. 2020.
- [7] W. Shin, M. Vaezi, B. Lee, D. J. Love, J. Lee, and H. V. Poor, "Non-orthogonal multiple access in multi-cell networks: Theory, performance, and practical challenges," *IEEE Communications Magazine*, vol. 55, no. 10, pp. 176–183, Oct. 2017, doi: 10.1109/MCOM.2017.1601065.
- [8] S. Donati, G. Mtini, and E. Randone, "Improving photodetector performance by means of microoptics concentrators," *Journal of Lightwave Technology*, vol. 29, no. 5, pp. 661–665, 2011, doi: 10.1109/JLT.2010.2103302.
- [9] A. Benjebbour, Y. Saito, Y. Kishiyama, A. Li, A. Harada, and T. Nakamura, "Concept and practical considerations of non-orthogonal multiple access (NOMA) for future radio access," *ISAPCS 2013 - 2013 International Symposium on Intelligent Signal Processing and Communication Systems*, pp. 770–774, 2013, doi: 10.1109/ISAPCS.2013.6704653.
- [10] S. Sen, N. Santhapuri, R. R. Choudhury, and S. Nelakuditi, "Successive Interference Cancellation: A Back-of-the-Envelope Perspective," 2010.
- [11] G. Singh, A. Srivastava, and V. A. Bohara, "Impact of weather conditions and interference on the performance of VLC based V2V communication," *International Conference on Transparent Optical Networks*, vol. 2019-July, Jul. 2019, doi: 10.1109/ICTON.2019.8840164.
- [12] L. Guo et al., "You may also like Ultraviolet communication technique and its application Hadron-quark phase transition in the context of GW190814 Ishfaq A Rather, A A Usmani and S K Patra-A review of gallium nitride LEDs for multi-gigabit-per-second visible light data communications 20 Mb/s Experimental Demonstration Using Modulated 460 nm Blue LED for Underwater Wireless Optical Communications (UOWC)," *J. Phys*, p. 12069, 2021, doi: 10.1088/1742-6596/1878/1/012069.
- [13] S. Fuada, A. P. Putra, and T. Adiono, "Analysis of Received Power Characteristics of Commercial Photodiodes in Indoor Los Channel Visible Light Communi... Analysis of Received Power Characteristics of Commercial Photodiodes in Indoor Los Channel Visible Light Communication," (*IJACSA International Journal of Advanced Computer Science and Applications*, vol. 8, no. 7, 2017, Accessed: Jun. 08, 2022. [Online]. Available: www.ijacsa.thesai.org
- [14] M. Basha, M. J. Sibley, and P. J. Mather, "Design and implementation of a long range indoor VLC system using PWM," *Annals of Emerging Technologies in Computing*, vol. 3, no. 1, pp. 20–27, Jan. 2019, doi: 10.33166/AETIC.2019.01.003.
- [15] M. Z. Win, P. C. Pinto, and L. A. Shepp, "A mathematical theory of network interference and its applications," *Proceedings of the IEEE*, vol. 97, no. 2, pp. 205–230, 2009, doi: 10.1109/JPROC.2008.2008764.
- [16] Y. Liu, Z. Qin, M. El-kashlan, Z. Ding, A. Nallanathan, and L. Hanzo, "Non-Orthogonal Multiple Access for 5G and Beyond," *Proceedings of the IEEE*, vol. 105, no. 12, pp. 2347–2381, Aug. 2018, doi: 10.48550/arxiv.1808.00277.
- [17] A. Naeem, N. U. Hassan, M. A. Pasha, C. Yuen, and A. Sikora, "Performance analysis of TDOA-based indoor positioning systems using visible LED Lights," *Proceedings of the 2018 IEEE 4th International Symposium on Wireless Systems within the International Conferences on Intelligent Data Acquisition and Advanced Computing Systems, IDAACS-SWS 2018*, pp. 103–107, Nov. 2018, doi: 10.1109/IDAACS-SWS.2018.8525567.
- [18] M. Doniec, I. Vasilescu, M. Chitre, C. Detweiler, M. Hoffmann-Kuhnt, and D. Rus, "AquaOptical: A lightweight device for high-rate long-range underwater point-to-point communication," *MTS/IEEE Biloxi - Marine Technology for Our Future: Global and Local Challenges, OCEANS 2009, 2009*, doi: 10.23919/OCEANS.2009.5422200.
- [19] Q. Li, T. Shang, T. Tang, and Z. Dong, "Optimal Power Allocation Scheme Based on Multi-Factor Control in Indoor NOMA-VLC Systems," *IEEE Access*, vol. 7, pp. 82878–82887, 2019, doi: 10.1109/ACCESS.2019.2924027.

- [20] S. Tao, H. Yu, Q. Li, and Y. Tang, "Performance analysis of gain ratio power allocation strategies for non-orthogonal multiple access in indoor visible light communication networks," *Eurasip Journal on Wireless Communications and Networking*, vol. 2018, no. 1, pp. 1–14, Dec. 2018, doi: 10.1186/S13638-018-1152-Z/FIGURES/5.
- [21] F. Wang, C. Xu, and Y. Zhang, "A new modulation scheme for IR-UWB communication systems," *Journal of Electronics*, vol. 26, no. 4, pp. 497–502, 2009, doi: 10.1007/S11767-008-0075-Y.
- [22] G. Wang, J. Zhao, L.-K. Chen, and Y. Shao, "Improved joint subcarrier and power allocation to enhance the throughputs and user fairness in indoor OFDM-NOMA VLC systems," *Optics Express*, Vol. 29, Issue 18, pp. 29242–29256, vol. 29, no. 18, pp. 29242–29256, Aug. 2021, doi: 10.1364/OE.440735.
- [23] N. Anous, M. Abdallah, M. Uysal, and K. Qaraqe, "Performance Evaluation of LOS and NLOS Vertical Inhomogeneous Links in Underwater Visible Light Communications," *IEEE Access*, vol. 6, pp. 22408–22420, Mar. 2018, doi: 10.1109/ACCESS.2018.2815743.
- [24] Z. Ghassemlooy, W. Popoola, and S. Rajbhandari, *Optical wireless communications: system and channel modelling with Matlab*. CRC press, 2019.
- [25] J. A. Anguita, I. B. Djordjevic, M. A. Neifeld, and B. v. Vasic, "Shannon capacities and error-correction codes for optical atmospheric turbulent channels," *Journal of Optical Networking*, Vol. 4, Issue 9, pp. 586–601, vol. 4, no. 9, pp. 586–601, Sep. 2005, doi: 10.1364/JON.4.000586.